Published OnlineFirst August 13, 2014; DOI: 10.1158/1535-7163.MCT-14-0451

Small Molecule Therapeutics

Molecular Cancer Therapeutics

Synergistic Simvastatin and Metformin Combination Chemotherapy for Osseous Metastatic Castration-Resistant Prostate Cancer

Melissa A. Babcook[1,2], Sanjeev Shukla[1], Pingfu Fu[3], Edwin J. Vazquez[4], Michelle A. Puchowicz[2,4], Joseph P. Molter[5], Christine Z. Oak[6], Gregory T. MacLennan[7], Chris A. Flask[5], Daniel J. Lindner[8], Yvonne Parker[8], Firouz Daneshgari[1], and Sanjay Gupta[1,2,9]

Abstract

Docetaxel chemotherapy remains a standard of care for metastatic castration-resistant prostate cancer (CRPC). Docetaxel modestly increases survival, yet results in frequent occurrence of side effects and resistant disease. An alternate chemotherapy with greater efficacy and minimal side effects is needed. Acquisition of metabolic aberrations promoting increased survival and metastasis in CRPC cells includes constitutive activation of Akt, loss of adenosine monophosphate-activated protein kinase (AMPK) activity due to Ser-485/491 phosphorylation, and overexpression of 3-hydroxy-3-methylglutaryl–Coenzyme A reductase (HMG-CoAR). We report that combination of simvastatin and metformin, within pharmacologic dose range (500 nmol/L to 4 μmol/L simvastatin and 250 μmol/L to 2 mmol/L metformin), significantly and synergistically reduces C4-2B3/B4 CRPC cell viability and metastatic properties, with minimal adverse effects on normal prostate epithelial cells. Combination of simvastatin and metformin decreased Akt Ser-473 and Thr-308 phosphorylation and AMPKα Ser-485/491 phosphorylation; increased Thr-172 phosphorylation and AMPKα activity, as assessed by increased Ser-79 and Ser-872 phosphorylation of acetyl-CoA carboxylase and HMG-CoAR, respectively; decreased HMG-CoAR activity; and reduced total cellular cholesterol and its synthesis in both cell lines. Studies of C4-2B4 orthotopic NCr-*nu*/*nu* mice further demonstrated that combination of simvastatin and metformin (3.5–7.0 μg/g body weight simvastatin and 175–350 μg/g body weight metformin) daily by oral gavage over a 9-week period significantly inhibited primary ventral prostate tumor formation, cachexia, bone metastasis, and biochemical failure more effectively than 24 μg/g body weight docetaxel intraperitoneally injected every 3 weeks, 7.0 μg/g/day simvastatin, or 350 μg/g/day metformin treatment alone, with significantly less toxicity and mortality than docetaxel, establishing combination of simvastatin and metformin as a promising chemotherapeutic alternative for metastatic CRPC. *Mol Cancer Ther; 13(10); 1–15. ©2014 AACR.*

Introduction

The recurrence and/or progression of castration-resistant prostate cancer (CRPC) following androgen deprivation therapy (ADT) is diagnosed by rising serum PSA and appearance of primarily osseous metastases (1). In the United States, approximately 30,000 men die each year from metastatic CRPC (mCRPC), a majority of them succumbing to metastasis- and treatment-related complications (2). Docetaxel is the most commonly prescribed first-line chemotherapy for mCRPC (2). Although docetaxel provides a modest (2.4-month) increase in median overall survival, many patients with mCRPC cannot tolerate this cytotoxic chemotherapy due to advanced age, medical comorbidities, or limited bone marrow reserves (3). Most patients receiving docetaxel eventually discontinue use due to the development of docetaxel-resistant disease (3). Other recently FDA-approved treatments for mCRPC include sipuleucel-T, cabazitaxel, and abiraterone; however, these expensive treatment modalities only provide a median survival benefit of 2 to 5 months (1–4). The identification of an effective, low-cost alternate chemotherapy with fewer side effects may lead to increased survival and greatly benefit quality of life of patients.

[1]Department of Urology, Case Western Reserve University, and The Urology Institute, University Hospitals Case Medical Center, Cleveland, Ohio. [2]Department of Nutrition, Case Western Reserve University, Cleveland, Ohio. [3]Department of Epidemiology and Biostatistics, Case Western Reserve University, Cleveland, Ohio. [4]Mouse Metabolic Phenotyping Center, Analytical and Metabolic Core, Case Western Reserve University, Cleveland, Ohio. [5]Imaging Research Core Facility, Case Western Reserve University, Cleveland, Ohio. [6]Department of Biology, Case Western Reserve University, Cleveland, Ohio. [7]Department of Pathology, Case Western Reserve University, Cleveland, Ohio. [8]Department of Cancer Biology, Cleveland Clinic Foundation, Cleveland, Ohio. [9]Division of General Medical Sciences, Case Comprehensive Cancer Center, Cleveland, Ohio.

Note: Supplementary data for this article are available at Molecular Cancer Therapeutics Online (http://mct.aacrjournals.org/).

Corresponding Author: Sanjay Gupta, Case Western Reserve University, 10900 Euclid Avenue, Cleveland, OH 44106. Phone: 216-368-6162; Fax: 216-368-0213; E-mail: sanjay.gupta@case.edu

doi: 10.1158/1535-7163.MCT-14-0451

Published OnlineFirst August 13, 2014; DOI: 10.1158/1535-7163.MCT-14-0451

Metabolic aberrations promoting survival and metastasis have been identified in human CRPC bone metastasis specimens. These include increased protein expression of 3-hydroxy-3-methylglutaryl-Coenzyme A reductase (HMG-CoAR, the mevalonate pathway rate-limiting enzyme dominant in cholesterol, isoprenoid, and androgen synthesis) and reduced activity of 5′-adenosine monophosphate-activated protein kinase (AMPK, the primary enzyme regulating cellular energy homeostasis) and significantly elevated levels of cholesterol and fatty acids (5). In addition, high-intensity immunostaining of prostate cancer specimens for p-Akt and low-intensity staining for p-ERK are predictive of progression to castration resistance (6), and PTEN deletion occurs in 70% of human specimens during advanced-stage CRPC (7). PTEN dephosphorylates phosphatidylinositol (3, 4, 5)-trisphosphate (PIP3), inhibiting Akt recruitment to the plasma membrane and activation; PTEN deletion leads to constitutively active Akt.

A growing body of evidence suggests that hypercholesterolemia and type 2 diabetes (T2D) are correlated with increased cancer progression. Hypercholesterolemia and T2D are frequently present as comorbidities associated with obesity (8), and both are associated with an increased risk of developing advanced prostate cancer (9–12). Statins directly inhibit HMG-CoAR activity by binding its active site and are approved for treatment of hypercholesterolemia (13). Metformin, an indirect activator of AMPKα, is approved by the FDA for the treatment of T2D (14). Use of lipophilic statins or metformin has been associated with reduced risk of advanced prostate cancer and shown to reduce the probability of biochemical failure, recurrence, and death from mCRPC, after surgery and radiotherapy (15–20). Lehman and colleagues (21) demonstrated in a T2D population that, among nonstatin users, the predictive prostate cancer HR for metformin use versus sulfonylurea (an antidiabetic drug that stimulates insulin release from pancreatic beta cells) use was 2.15 [95% confidence interval (CI), 1.83–2.52], and among sulfonylurea users, the HR for statin use was 0.60 (95% CI, 0.49–0.70); however, T2D patients taking both metformin and statin had greatly reduced incidence of prostate cancer (HR 0.32; 95% CI, 0.25–0.42) compared with T2D patients taking neither medication. Individually, lipophilic statins and metformin have shown effectiveness in the inhibition of cell-cycle progression, proliferation, and metastatic properties and the induction of cell death in androgen-refractory human prostate cancer PC-3 and DU145 cells in both *in vitro* and xenograft models (22–26). Moreover, treatment of prostate cancer cells with statins or metformin has been shown to decrease Akt phosphorylation and activity (19, 24). Therefore, given the metabolic aberrations present in mCRPC, and that simvastatin inhibits HMG-CoAR and Akt activity while metformin inhibits Akt and activates AMPKα, we hypothesize that combination of simvastatin and metformin could synergistically inhibit osseous mCRPC in both *in vitro* and *in vivo* models.

Materials and Methods

Cell culture and treatment

All reagents were purchased from Fisher Scientific, unless otherwise noted. C4-2B3, B4, and B5 cells were obtained in January 2012 from Dr. R.A. Sikes (University of Delaware, Newark, DE); PC-3 D12 cells were a gift from Dr. R.W. Watson (University College Dublin, Dublin, Ireland), obtained in February 2012; MDA-MB-231 cells were a gift from Dr. H.-Y. Kao (Case Western Reserve University, Cleveland, OH), obtained in July 2012; and MDA-MB-231(SA) cells were a gift from Dr. T. Guise (Indiana University, Indianapolis, IN), obtained in October 2012. These cell lines were established in the laboratory of the donors with published reference and were not authenticated by the recipient. These cell lines were obtained from donor laboratory at passages 2 to 3, propagated by our laboratory and frozen at −150°C until use, and all experiments were performed using passages 5 to 15. Normal human prostate epithelial PrEC cells were purchased from Clonetics in March 2009, which authenticates cell lines using immunostaining, morphology, and flow cytometry. Transformed prostate epithelial RWPE1 cells and human prostate cancer LNCaP cells were purchased from the ATCC in June 2011 and authenticated using short tandem repeat profiling. These cell lines were frozen at −150°C until propagation in January 2012, and experimentation was done using passages 2 to 4 for PrEC and passages 5 to 15 for RWPE-1 and LNCaP cells. The cells were grown in appropriate culture medium containing 1% penicillin–streptomycin in a humidified 5% CO_2 at 37°C. For the demonstration of Akt constitutive activation, C4-2B3/B4 cells were switched to serum-free RPMI-1640 overnight and treated with 100 to 300 ng/mL recombinant human (hrIGF-1; Gibco Life Technologies), representative of the low end and high end of the normal physiologic plasma range in men ≥50 years of age, and 2 μmol/L Akt Inhibitor VIII (Santa Cruz Biotechnology). Cells were treated with docetaxel concentrations ranging from 1 nmol/L to 10 μmol/L for 24 hours to simulate pharmacologic plasma levels in patients with metastatic prostate cancer treated with 75 to 100 mg/m^2 intravenously, with a plasma C_{max} of 5 to 10 μmol/L within 1 hour, diminishing to C_{min} = 1 to 10 nmol/L 24 hours after treatment (27). Cells were treated with activated simvastatin and metformin (AK Scientific Inc.), alone or in combination, for 96 hours to simulate chronic daily use, at concentrations corresponding to pharmacologic plasma ranges for hypercholesterolemic and T2D patients.

Simvastatin activation

The prodrug simvastatin was activated to simvastatin acid before *in vitro* and *in vivo* use, as per the manufacturer's protocol, neutralized (pH = 7.3), and filter sterilized. More than 93% lactone-to-acid conversion was confirmed by electron ionization (EI)–gas chromatography–mass spectroscopy (GC/MS). Stock solution was stored at 4°C and prepared fresh every 90 days.

Published OnlineFirst August 13, 2014; DOI: 10.1158/1535-7163.MCT-14-0451

Methylene blue assay

Cells were cultured in 24-well plates; following treatment, cells were washed with PBS, stained with 2 g/L methylene blue solution for 1 hour, and excess stain was removed with ddH_2O. Plates were examined under light microscope and photographed. For semiquantification, bound methylene blue was eluted with 0.1 N HCl with shaking, and absorbance was measured spectrophotometrically at $\lambda = 650$ nm (FLUOstar Omega; BMG LabTech).

Total and free cholesterol estimation

Cholesterol levels were measured by GC/MS using a protocol modified from Bederman and colleagues (28). Details are provided in the Supplementary Materials and Methods section.

Western blotting

Lysates of exponentially growing cells and of mouse ventral prostate tissue were prepared by homogenization using stainless steel beads (Next Advance), as described previously (29). Protein (40 μg) was denatured at 95°C, resolved over 4% to 20% SDS-PAGE (Bio-Rad), and transferred to a nitrocellulose membrane. Following Ponceau S visualization and blocking with 5% nonfat dry milk TBST, pH 7.4 (USB) for 1 hour, the membrane was probed with primary antibody overnight at 4°C (Supplementary Table S1), incubated with corresponding horseradish peroxidase–conjugated secondary antibody (Santa Cruz Biotechnology), and detected using Pierce ECL reagent. Bands were visualized upon autoradiography film (Denville Scientific) exposure and quantitated using the ImageJ software (NIH).

Synergistic quantification of drug combination

Synergistic action of drug in combination was performed as per the Chou–Talalay method using CompuSyn software (30).

Cell migration assay

Two-dimensional cell motility was examined by the scratch assay (31). Photographic images were captured using digital camera Zeiss Telaval 31 light microscope (Carl Zeiss) at ×25 magnification connected to SPOT Insight Color Digital Camera Model 3.2.0 and SPOT Basic imaging software (SPOT Imaging Solutions). ImageJ was used to calculate scratch area.

Invasion assay

Invasion assay was performed using a 24-well hanging insert (Millipore) precoated with Matrigel Matrix (BD Biosciences), as previously described (32).

Anchorage-independent cell growth assay

An anchorage-independent assay in C4-2B3/B4 cells was performed, as previously described (33).

Cholesterol synthesis by D_2O incorporation

De novo cholesterol synthesis was estimated by published procedure with modification (28, 34). Details are provided in the Supplementary Materials and Methods section.

Blood glucose estimation

Blood glucose (mg/dL) was measured using a TRUEresult meter (CVS Pharmacy) and TRUEtest test strips (Chinook Diabetics).

Plasma alanine aminotransferase measurement

Plasma alanine aminotransferase (ALT) was measured using an enzymatic kinetic spectrophotometric kit (Sekisui Diagnostics LLC) according to the manufacturer's instructions.

Plasma PSA estimation

Plasma PSA was measured by ELISA (Abnova) as per the manufacturer's instructions using FLUOstar Omega spectrophotometer.

Quantitation of simvastatin acid and metformin in plasma and ventral prostate

Concentration of simvastatin acid and metformin was determined by GC/MS using modified protocols (35–37). Details are provided in the Supplementary Materials and Methods section.

Animal studies

Animal experiments using male NCr-nu/nu mice were performed in accordance with recommendations of the Guide for the Care and Use of Laboratory Animals of the NIH, and protocol was approved by the CWRU School of Medicine Institutional Animal Care and Use Committee. Details are provided in the Supplementary Materials and Methods section.

Metastasis examination

Spinal column and femur metastases were examined using X-ray imaging. Mice were anesthetized with 2% isoflurane, and X-rays were obtained at 34 kV and 500 μA for a 6-second integration time. Images were captured on a Rad-Icon digital detector with Shadow Cam software. Cachexic mice and mice with palpable primary tumors were monitored with sequential X-ray images. All X-ray images were evaluated by a radiologist, and areas of suspected metastasis within spinal column and femurs were noted.

Histologic analysis

Mouse ventral prostate and primary tumors, spinal columns, femurs, rectus femoris muscle, and left lateral liver lobe tissues were fixed with 10% (w/v) phosphate-buffered formalin followed by bone decalcification and paraffin embedding. Sections (5 μm) were stained with hematoxylin and eosin (H&E). Spinal column and femur slides were immunostained using human-specific anti–androgen receptor antibody (Cell Signaling Technology; #5153) and evaluated by a pathologist.

Published OnlineFirst August 13, 2014; DOI: 10.1158/1535-7163.MCT-14-0451

Statistical analysis

Quantitative values were represented as mean or median ± SD or SEM of at least three independent experiments. Significance was determined by a two-tailed, unpaired Student *t* test, Kruskal–Wallis test, or ANOVA, followed by the Tukey multiple comparison procedure (SAS 9.3). *, $P < 0.05$; **, $P < 0.01$; ***, $P < 0.001$. Comparisons resulting in $P < 0.05$ were considered statistically significant.

Results

C4-2B cell lines as model for osseous mCRPC

In our studies, C4-2B3, C4-2B4, and C4-2B5 cell lines were used as *in vitro* models of osseous mCRPC. The C4-2B3-5 strains readily form large, poorly differentiated tumors with frequent (25%–37%) metastasis to the spinal column and femurs when orthotopically injected into castrated athymic mice (38). Metabolic aberrations in these cells include significantly increased protein expression of the 80- to 97-kDa full-length smooth endoplasmic reticulum membrane-bound glycoprotein and the approximately 65-kDa cleavage product of HMG-CoAR, which retains enzymatic activity within the cytoplasm, compared with PrEC cells. Furthermore, a complete lack of low-molecular-weight C-terminal cleavage products of HMG-CoAR, indicative of dysregulated negative-regulation and breakdown, was noted in these cells (Supplementary Fig. S1). This was associated with significantly elevated (2-fold) total cellular cholesterol (Supplementary Fig. S2). Consistent with a previous report (39), the free-to-total cellular cholesterol ratio was not affected by progression to castration resistance (attributed to unaltered cholesterol acyltransferase activity); approximately 80% to 95% of cellular cholesterol was in free form in all cell lines characterized, despite increase in total cellular cholesterol (Supplementary Fig. S3).

The C4-2B3-5 strains exhibit minimal ERK1/2 phosphorylation and constitutive activity of Akt (Supplementary Fig. S4A–S4C). In these cells, Akt phosphorylation is not affected by the presence or absence of FBS or by stimulation with human recombinant insulin-like growth factor-1. Significantly increased fatty acid and cholesterol were noted in clinical mCRPC specimens (5), indicative of inhibited AMPK activity. AMPK is a heterotrimeric protein consisting of a catalytic α subunit and two regulatory β and γ subunits (40, 41). Activation of AMPK involves AMP/ADP binding to γ-subunit regulatory sites, causing conformational changes to allosterically activate the α-subunit and allowing for α-subunit activation loop Thr-172 phosphorylation by upstream kinases (40, 41). Despite detectable p-Thr-172 AMPKα in C4-2B cell lines, AMPKα kinase activity is limited, as seen by reduced p-Ser-79 of acetyl-CoA carboxylase (ACC) and increased ACC protein expression (41 and Supplementary Fig. S4B). Akt-dependent inhibition of AMPKα activity, via Ser-485/491 phosphorylation of AMPKα_1/α_2, has been previously demonstrated in cardiac and skeletal muscle, brown adipose tissue, and granulosa cells (42–44). We hypothesized that constitutively active Akt may lead to inhibition of AMPKα activity in C4-2B3-5 cells. Using Akt Inhibitor VIII, we observed a marked decrease in p-Ser-485/491 AMPKα_1/α_2 and a concomitant increase in p-Thr-172 AMPKα and p-Ser-79 ACC, establishing the role of Akt in suppressing AMPKα activity in these cells (Supplementary Fig. S4D, lanes 3 and 7).

Combination of simvastatin and metformin synergistically inhibits C4-2B3/B4 cell viability

Docetaxel plasma concentrations, following chemotherapy, initially peak at 5 to 10 μmol/L within an hour, declining to ≤1 nmol/L within 24 hours (27). Treatment of C4-2B3/B4 cells with docetaxel in the pharmacologic range (1 nmol/L–10 μmol/L) for 24 hours led to decrease cell viability as an initial response followed by resistance to further viability inhibition by docetaxel after 100 nmol/L concentration. Docetaxel treatment also causes a significant adverse effect on the viability of PrEC cells (Fig. 1A). In contrast, 1:500 simvastatin and metformin combination treatment for 96 hours [time point chosen from individual dose–response curves for simvastatin and metformin (Supplementary Fig. S5) and synergy determination per the Chou–Talalay method; Supplementary Materials and Methods; Fig. 1B; Supplementary Fig. S6; Table 1, Supplementary Table S2] significantly decreased the viability of C4-2B3/B4 cells at 500 nmol/L to 4 μmol/L simvastatin and 250 μmol/L to 2 mmol/L metformin concentrations, with minimal effect on PrEC cells only at highest combination (Fig. 1C).

Combination of simvastatin and metformin inhibits metastatic potential of C4-2B3/B4 cells

Mortality and poor prognosis in patients with CRPC are related to metastasis of prostate cancer cells to bone and soft tissues (1, 2). Metabolic aberrations identified in mCRPC are intricately involved in enhanced tumor cell invasion and migration (45, 46). Accordingly, we assessed the potential of combining simvastatin and metformin to inhibit C4-2B3/B4 invasion, migration, and adhesion-independent cell growth metastatic properties. The effect of 1:500 combination of simvastatin and metformin on cell migration was assessed by the scratch assay and by allowing cells to migrate for 48 hours. As shown in Fig. 2A, a gradient of 1:500 simvastatin and metformin combination along the pharmacologic range significantly prevented wound closure over 48 hours in C4-2B3/B4 cells. In fact, simvastatin and metformin displayed significant dose reduction when used in combination; similar wound closure inhibition was observed with 1 μmol/L simvastatin + 500 μmol/L metformin combination, as was seen with 4 μmol/L simvastatin or 2 mmol/L metformin treatment individually. In contrast to individual treatment with 4 μmol/L simvastatin or 2 mmol/L metformin for 48 hours, which inhibited wound closure by 43% and 30% in C4-2B3 and 58% and 49% in C4-2B4 cells, respectively, 4 μmol/L simvastatin + 2 mmol/L metformin combination completely prevented scratch closure after 48-hour treatment in both cell lines.

Published OnlineFirst August 13, 2014; DOI: 10.1158/1535-7163.MCT-14-0451

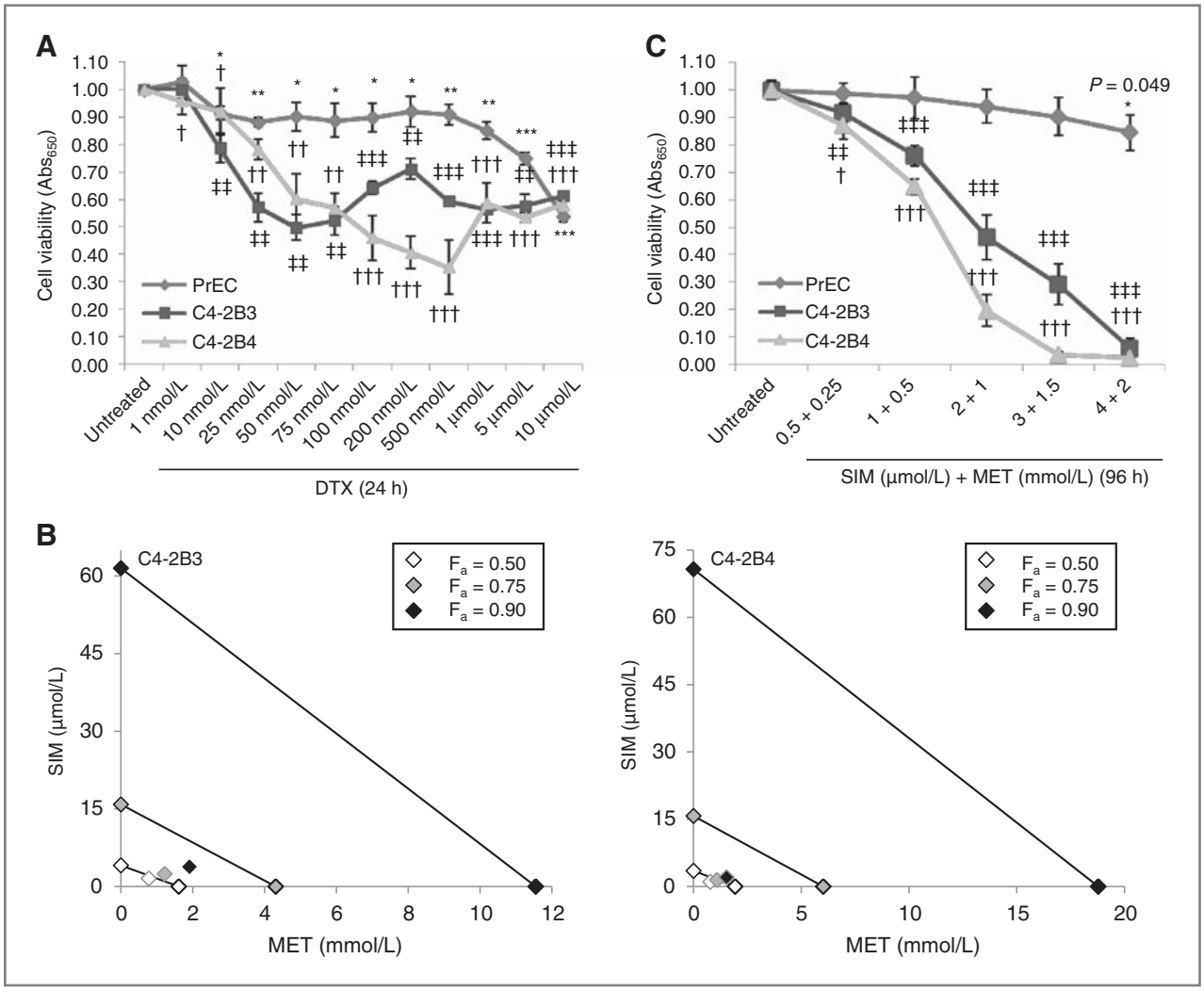

Figure 1. Combination of simvastatin (SIM) and metformin (MET) synergistically inhibits mCRPC cell viability more effectively than docetaxel, with minimal adverse viability effect on PrEC normal prostate epithelial cells. A, quantification (mean ± SD) of cell viability by methylene blue staining after docetaxel treatment (24 hours) over pharmacologic range (1 nmol/L–10 μmol/L) in PrEC, C4-2B3, and C4-2B4 cells. $n \geq 3$ per group. B, classic isobolograms for (1:500) combination (96 hours) at IC_{50}, IC_{75}, and IC_{90} for C4-2B3 and C4-2B4, respectively. Points below the "lines of additivity" indicate synergism. C, quantification (mean ± SD) of cell viability by methylene blue staining following treatment with (1:500) combination of simvastatin and metformin (96 hours) over the pharmacologic range (500 nmol/L–4 μmol/L simvastatin and 250 μmol/L–2 mmol/L metformin) in PrEC, C4-2B3, and C4-2B4 cells. $n \geq 3$ per group. *, †, ‡, $P < 0.05$; **, ††, ‡‡, $P < 0.01$; and ***, †††, ‡‡‡, $P < 0.001$, compared with untreated control determined by the two-tailed Student t test. *, **, ***, significance corresponds to PrEC; †, ††, †††, significance corresponds to C4-2B4; and ‡, ‡‡, ‡‡‡, significance corresponds to C4-2B3 cell line.

We also determined adhesion-independent cell growth by soft-agar colony formation. The number of colonies observed per 2-mm field after 10 days was significantly fewer when pretreated with 4 μmol/L simvastatin + 2 mmol/L metformin combination compared with untreated control, 4 μmol/L simvastatin or 2 mmol/L metformin alone (Fig. 2B). In addition, invasion was assessed by Transwell assay, in which C4-2B3/B4 cells were pretreated for 96 hours, then cells were given opportunity to invade through a Matrigel-coated Transwell toward serum-free or 10% FBS media stimulation for 48 hours. C4-2B3/B4 cells demonstrate highly invasive character; 36% to 40% cells cross the Matrigel-coated transwell even in the absence of FBS-invasive stimulation conditions (Fig. 2C). The combination of 4 μmol/L simvastatin + 2 mmol/L metformin was significantly more effective in the inhibition of C4-2B3/B4 invasion compared with untreated control, 4 μmol/L simvastatin or 2 mmol/L metformin treatment individually.

Combination of simvastatin and metformin treatment ameliorates metabolic aberrations in C4-2B3/B4 cells

Next, we sought to determine whether simvastatin and metformin combination (1:500) mitigates metabolic aberrations observed in C4-2B3/B4 cells. Treatment of cells with 4 μmol/L simvastatin and 2 mmol/L metformin combination decreased Thr-308 and Ser-473 phosphorylation of Akt

Published OnlineFirst August 13, 2014; DOI: 10.1158/1535-7163.MCT-14-0451

Table 1. Simvastatin (SIM) and metformin (MET) combination (1:500) synergistically inhibits cell viability in C4-2B3 and C4-2B4 CRPC cell lines

Cell lines	Treatment	Parameters			CI value				DRI value			
		m	r	D_m	IC_{50}	IC_{75}	IC_{90}	IC_{95}	IC_{50}	IC_{75}	IC_{90}	IC_{95}
C4-2B3	SIM	0.81 ± 0.11	0.983	4.09 μmol/L					2.63	6.51	16.1	29.8
	MET	1.12 ± 0.09	0.994	1.61 mmol/L					2.07	3.54	6.05	8.71
	Combination (1:500)	3.24 ± 0.64	0.964	1.21 μmol/L SIM + 610 μmol/L MET	0.862	0.436	0.227	0.148				
C4-2B4	SIM	0.73 ± 0.16	0.958	3.50 μmol/L					3.37	10.8	34.6	76.5
	MET	0.97 ± 0.11	0.986	1.93 mmol/L					2.48	5.52	12.3	21.1
	Combination (1:500)	2.44 ± 0.29	0.973	1.55 μmol/L SIM + 780 μmol/L MET	0.699	0.274	0.110	0.060				

NOTE: Slope (m), correlation coefficients (r), and median-effect dosages (D_m) from median-effect plots for SIM alone, MET alone, and (1:500) SIM + MET combination treatment for 96 h, and combination indexes (CI) and dose-reduction indexes (DRI) at the fraction of cells affected by treatment (f_a) = 0.50, 0.75, 0.90, and 0.95 for (1:500) SIM + MET combination treatment for 96 h in C4-2B3 and C4-2B4 cells.

at an earlier time point (by 24 hours) and more effectively than either drug alone; suppression of Akt phosphorylation continued throughout the duration (Fig. 3A). Combination treatment also decreased inhibitory p-Ser-485/491 AMPKα_1/α_2, and concomitantly increased p-Thr-172 AMPKα and AMPKα kinase activity, with notable increase in Ser-79 ACC and Ser-872 HMG-CoAR phosphorylation. Simvastatin and metformin combination treatment modestly decreased ACC protein expression at 48 and 72 hours in C4-2B3/B4 cells, compared with untreated controls. Protein expression of the 80- to 97-kDa full-length HMG-CoAR glycoprotein remained relatively unchanged, whereas expression of the approximately 65-kDa HMG-CoAR cleavage product clearly increased following simvastatin and metformin combination treatment in both C4-2B3/B4 cells, compared with untreated, 4 μmol/L simvastatin or 2 mmol/L metformin alone. Despite this, treatment of C4-2B3/B4 cells with 4 μmol/L simvastatin + 2 mmol/L metformin combination for 48 hours significantly reduced total cellular cholesterol compared with untreated control (56% and 35% decrease in C4-2B3/B4, respectively; Fig. 3B), restoring cholesterol concentrations within C4-2B3/B4 to approximately those of RWPE-1 cells (Supplementary Fig. S2C), and significantly reduced HMG-CoAR activity as determined by quantization of *de novo* cholesterol synthesis by deuterium incorporation (74% and 53% reduction in *de novo* cholesterol synthesis in C4-2B3/B4 cells, respectively; Fig. 3C; Supplementary Fig. S7; ref. 47). Therefore, an increase in HMG-CoAR expression is likely to compensate for direct and indirect HMG-CoAR enzymatic inhibition by simvastatin and metformin.

Combination of simvastatin and metformin significantly inhibits primary tumor growth and metastasis in a mouse model of CRPC

To demonstrate the *in vivo* efficacy of the combination of simvastatin and metformin for the treatment of CRPC, castrated male NCr-*nu*/*nu* mice were orthotopically inoculated with C4-2B4 cells within the ventral prostate. Tumors were allowed to seed for a week, followed by 9 weeks of simvastatin and metformin treatment (Supplementary Materials and Methods and Supplementary Fig. S8). Orthotopic implantation of C4-2B4 cells resulted in poorly differentiated primary tumor formation in 90% of animals (Fig. 4A and Supplementary Fig. S9), cachexia in 20% of animals, significantly increased genitourinary (GU) tract weight (Fig. 4B), increased ventral prostate proliferative index (Fig. 4C), biochemical failure determined by readily detectable PSA (Fig. 4D), metastasis to spinal column and femurs in 20% of animals (Fig. 5A), and premature animal death ($n = 2$ mice sacrificed early). No soft-tissue metastases were observed in any treatment group. Simvastatin or metformin individual treatments reduced the incidence of primary ventral prostate tumor (38% and 44% of mice, respectively). Ventral prostate/primary tumor histopathology in the simvastatin and metformin groups ranged from high-grade prostatic intraepithelial neoplasia (HGPIN) to poorly differentiated high-grade tumors, similar to those observed in the control group (Fig. 4A and Supplementary Fig. S9). Individual treatment with simvastatin or metformin did not significantly decrease GU tract weight or ventral prostate/primary tumor proliferative index compared with untreated controls (Fig. 4B and C). However, the simvastatin group demonstrated a significant decrease in the plasma PSA versus untreated control, consistent with previous reports (24, 48); metformin treatment did not affect plasma PSA (Fig. 4D). Simvastatin and metformin individual treatment led to slightly reduced cachexia incidence (13% and 11% of mice, respectively). Two untreated mice, who also displayed cachexia, were determined to have femoral bone metastases (Fig. 5A). Although only one mouse in the simvastatin group showed signs of cachexic wasting, two mice—the cachexic mouse and another, both with large primary tumors—presented with bone metastases; the

Published OnlineFirst August 13, 2014; DOI: 10.1158/1535-7163.MCT-14-0451

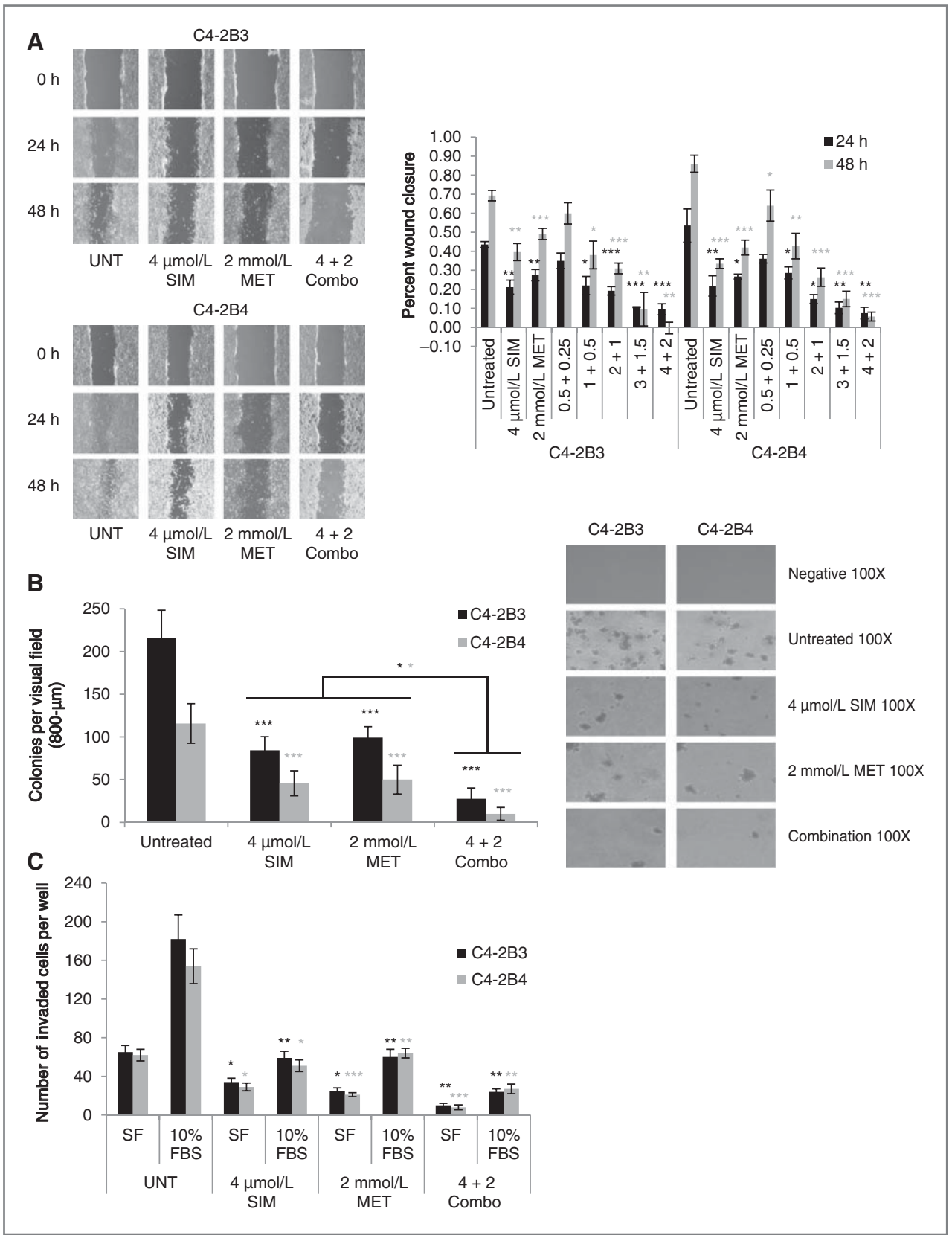

Published OnlineFirst August 13, 2014; DOI: 10.1158/1535-7163.MCT-14-0451

cachexic mouse had metastases within the lumbar vertebrae, and the second mouse presented with femoral head metastases (Fig. 5A). In our studies, simvastatin did not prevent progression to metastatic disease. Despite similar incidence of primary tumor and cachexia as the simvastatin group, no bone metastases were identified in any mouse within the metformin group (Fig. 5B). Treatment with 24 μg/g body weight/day docetaxel every 3 weeks for 3 cycles resulted in the inhibition of primary tumor growth (Fig. 4A and Supplementary Fig. S9), yet caused toxicity, intestinal blockage, and mortality of 75% of mice (Supplementary Fig. S10). Of the two mice surviving to the end of the 9-week experiment, one displayed normal ventral prostate histology with no noted metastases and the other had HGPIN with small femur metastasis (Figs. 4A and 5A). Docetaxel did not significantly reduce GU tract weight, ventral prostate proliferative index, or plasma PSA concentration compared with the control group (Fig. 4B–D). In sharp contrast, high-dose (HD) or low-dose (LD) simvastatin and metformin combination completely inhibited primary ventral prostate tumor growth (no primary tumors detected in either treatment group); all HD and LD group mice had normal prostate glandular structure with reduced GU tract weight (Fig. 4A and B; Supplementary Fig. S9). HD and LD combination significantly reduced proliferation in the ventral prostate tissue assessed through PCNA proliferative index (Fig. 4C), and prevented biochemical failure, evidenced by undetectable plasma PSA (Fig. 4D). HD and LD combination treatment completely eliminated incidence of cachexic wasting and prevented bone metastasis (Fig. 5B). Also of importance, no HD or LD group mice demonstrated any apparent signs of toxicity from treatment, as determined by the monitoring of body weight (Supplementary Fig. S10), plasma ALT (Supplementary Fig. S11) liver, and muscle histology or mortality (Supplementary Fig. S12 and S13). The *in vivo* results suggest that HD and LD combination treatment is significantly more effective and less toxic than docetaxel in the inhibition of CRPC progression and metastasis.

Combination of simvastatin and metformin lowers plasma cholesterol and blood glucose and are bioavailable within plasma and prostate

Next, we determined whether combination of simvastatin and metformin was efficacious in reducing plasma cholesterol and blood glucose, and if simvastatin and metformin were bioavailable within the plasma and ventral prostate. Animals were orally gavaged daily with β-hydroxyacid simvastatin, the same activated simvastatin was used within the *in vitro* experiments, to prevent the need for cytochrome P450 isoform 3A4 (CYP3A4)–humanized mice. Activated simvastatin is approximately 93.7% simvastatin acid (Supplementary Fig. S14). The concentration of simvastatin β-hydroxyacid and metformin was quantified by EI–GC/MS (Supplementary Materials and Methods and Supplementary Fig. S15–S23). Both simvastatin acid and metformin were readily detectable at appreciable concentrations in the plasma of respectively treated groups collected terminally 1 to 8 hours after gavage (Supplementary Table S3). As expected, simvastatin acid and metformin treatment lowered both plasma cholesterol and blood glucose to varying degrees. By 2 weeks after treatment initiation, metformin, LD, and HD treatment lowered plasma cholesterol, and by 4 weeks, both LD and HD combination treatment had significantly lowered plasma cholesterol concentration compared with untreated, simvastatin, metformin, and docetaxel treatment groups (Fig. 6A). Plasma cholesterol remained lower within the simvastatin and HD groups than untreated controls throughout the remainder of the experiment, albeit not statistically significant. Plasma cholesterol in metformin and LD groups significantly decreased initially at 4 weeks, but rebounded to levels comparable with untreated mice by 7 to 9 weeks. Lowering of blood glucose was noted by 2 weeks after treatment initiation, particularly and significantly in the metformin and HD groups, in which the blood glucose reduction was maintained throughout the 9-week experiment (Fig. 6B). Blood glucose was also lowered in simvastatin and LD groups 2 to 9 weeks following treatment initiation, but was not statistically significant.

Simvastatin acid and metformin were also bioavailable within the ventral prostate tissue (Supplementary Table S3). Surprisingly, terminal ventral prostate cholesterol concentration was significantly higher in the simvastatin and LD groups than in untreated controls, was significantly ($P < 0.001$) elevated in the HD group versus the untreated group, and also significantly greater than in simvastatin-, metformin-, and docetaxel-treated groups (Fig. 6C). Metformin or docetaxel treatment did not affect ventral prostate tissue cholesterol concentration. Representative ventral prostate tissue specimens from LD and HD groups demonstrated reduced Ser-473 and Thr-308 phosphorylation of Akt compared with untreated,

Figure 2. Combination of simvastatin (SIM) and metformin (MET) significantly inhibits metastatic properties of C4-2B3 and C4-2B4 mCRPC cells. A, representative images and quantification (mean ± SD) of cell migration by scratch assay (percent wound closure) following 24- and 48-hour treatment with untreated (UNT), 4 μmol/L simvastatin (IC_{50}), 2 mmol/L metformin (IC_{50}), and gradient (1:500) simvastatin + metformin combination in C4-2B3 and C4-2B4 cells. Scratch area at 0, 24, and 48 hours quantified from images using ImageJ software. $n = 3$ per group. *, $P < 0.05$; **, $P < 0.01$; and *** $P < 0.001$, compared with untreated control determined by the two-tailed Student *t* test. B, representative photographs and quantification (mean ± SD) of adhesion-independent cell growth by colony formation in soft agar in C4-2B3 and C4-2B4 cells. Cells were pretreated for 96 hours and then 1×10^4 cells grown in agar for 10 days before colonies per 2-mm visual field were counted. $n = 3$ per group. *, $P < 0.05$; and ***, $P < 0.001$, determined by ANOVA. C, quantification (mean ± SD) of C4-2B3 and C4-2B4 cellular invasion through Matrigel Transwell. Cells were pretreated for 96 hours with untreated, 4 μmol/L simvastatin (IC_{50}), 2 mmol/L metformin (IC_{50}), or (1:500) simvastatin + metformin combination, then 1×10^5 cells were seeded into top of Matrigel-coated Transwell and incubated for 48 hours; serum-free (SF) and 10% FBS RPMI-1640 media were used for invasion stimulus. $n = 3$ per group. *, $P < 0.05$; **, $P < 0.01$; and ***, $P < 0.001$, compared with respective serum-free– or 10% FBS-stimulated untreated control as determined by the two-tailed Student *t* test.

Published OnlineFirst August 13, 2014; DOI: 10.1158/1535-7163.MCT-14-0451

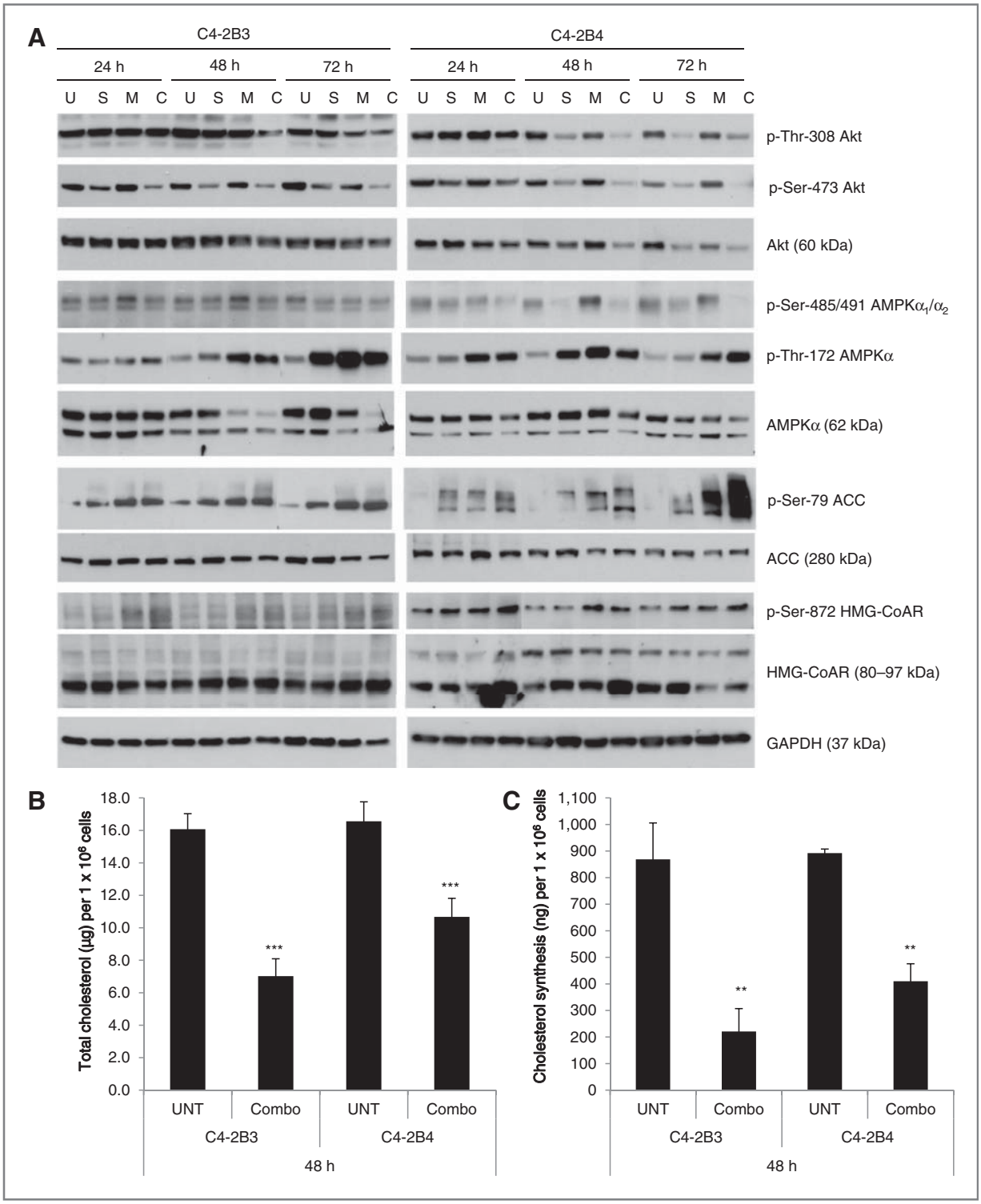

Figure 3. Combination of simvastatin (SIM) and metformin (MET) ameliorates metabolic aberrations of C4-2B3 and C4-2B4 mCRPC cells. A, Western blot analysis of Akt, AMPKα, ACC, and HMGCR phosphorylation and expression in C4-2B3 and C4-2B4 cells following 24, 48, and 72-hour treatment time course of untreated (U), 4 μmol/L simvastatin IC_{50} (S), 2 mmol/L metformin IC_{50} (M), or 4 μmol/L simvastatin + 2 mmol/L metformin combination (C). GAPDH was used as a loading control. B, quantification (mean ± SD) of total cholesterol (μg per 1×10^6 cells) following untreated (UNT) or 4 μmol/L simvastatin + 2 mmol/L metformin combination (combo) treatment for 48 hours in C4-2B3 and C4-2B4 cells as determined by EI-GC/MS. $n = 5$ per group. C, quantification (mean ± SD) of *de novo* cholesterol synthesis (ng per 1×10^6 cells) over 48 hours in untreated or 4 μmol/L simvastatin + 2 mmol/L metformin combination (Combo)–treated C4-2B3 and C4-2B4 cells as determined by deuterium incorporation and quantization by EI-GC/MS. $n = 5$ per group. **, $P < 0.01$ and ***, $P < 0.001$, compared with untreated control determined by the two-tailed Student *t* test.

Published OnlineFirst August 13, 2014; DOI: 10.1158/1535-7163.MCT-14-0451

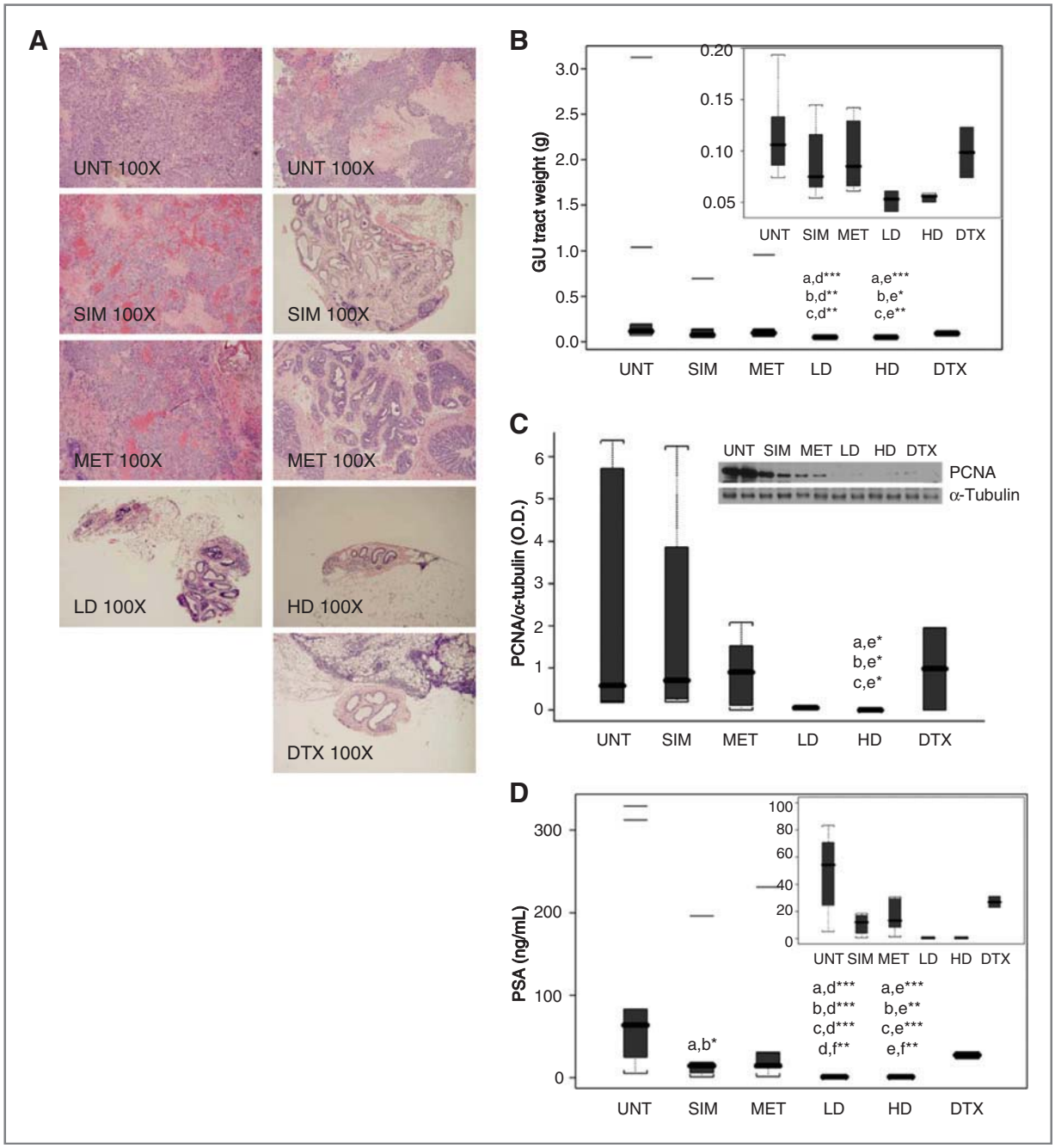

Figure 4. Combination of simvastatin (SIM) and metformin (MET) significantly inhibits prostate tumor progression in an orthotopic mouse model of CRPC. A, histopathology of representative mouse ventral prostates/tumors from six treatment groups. H&E staining, ×100 magnification. Slides were analyzed by a clinical pathologist (G.T. MacLennan). C4-2B4 xenografts produce poorly differentiated, highly vascularized tumors. Variation in treatment response with simvastatin and metformin groups, HGPIN to poorly differentiated tumors. Normal glandular structure in LD and HD treatment groups. B, mouse terminal GU tract weight (g) among six groups after 9-week treatment. Statistical difference was determined using the Kruskal–Wallis ANOVA followed by the Bonferroni multiple comparison procedure. Overall, a significant difference was found among six treatment groups ($P = 0.0002$). In pair-wise comparison, no significant differences were noted among the LD, HD, and docetaxel (DTX) treatment groups. C, Western blot analysis of proliferating cell nuclear antigen (PCNA) expression in representative ventral prostates from each group; α-tubulin was used as a loading control. Quantification of PCNA/α-tubulin (O.D.) ratio using ImageJ software. Statistical significance was determined by the Kruskal–Wallis ANOVA followed by the Tukey multiple comparison procedure. Overall, there was a significant difference among the six groups ($P = 0.022$). D, terminal plasma PSA (ng/mL) among the six groups. No PSA was detected in any plasma sample from LD or HD combination group; therefore, limits of detection (<0.75 ng/mL) used for statistical calculations. Statistical significance was determined by the Kruskal–Wallis ANOVA followed by the Tukey multiple comparison procedure. Overall, there was a significant difference in PSA concentration among the six treatment groups ($P \leq 0.0001$).HD, high-dose combination; LD, low-dose combination; UNT, untreated. Black bar, median; box, 25th to 75th percentiles; whiskers, range. Pair-wise comparisons were depicted where UNT (a), simvastatin (b), metformin (c), LD (d), HD (e), and docetaxel (f). *, $P < 0.05$; **, $P < 0.01$; and ***, $P < 0.001$.

Published OnlineFirst August 13, 2014; DOI: 10.1158/1535-7163.MCT-14-0451

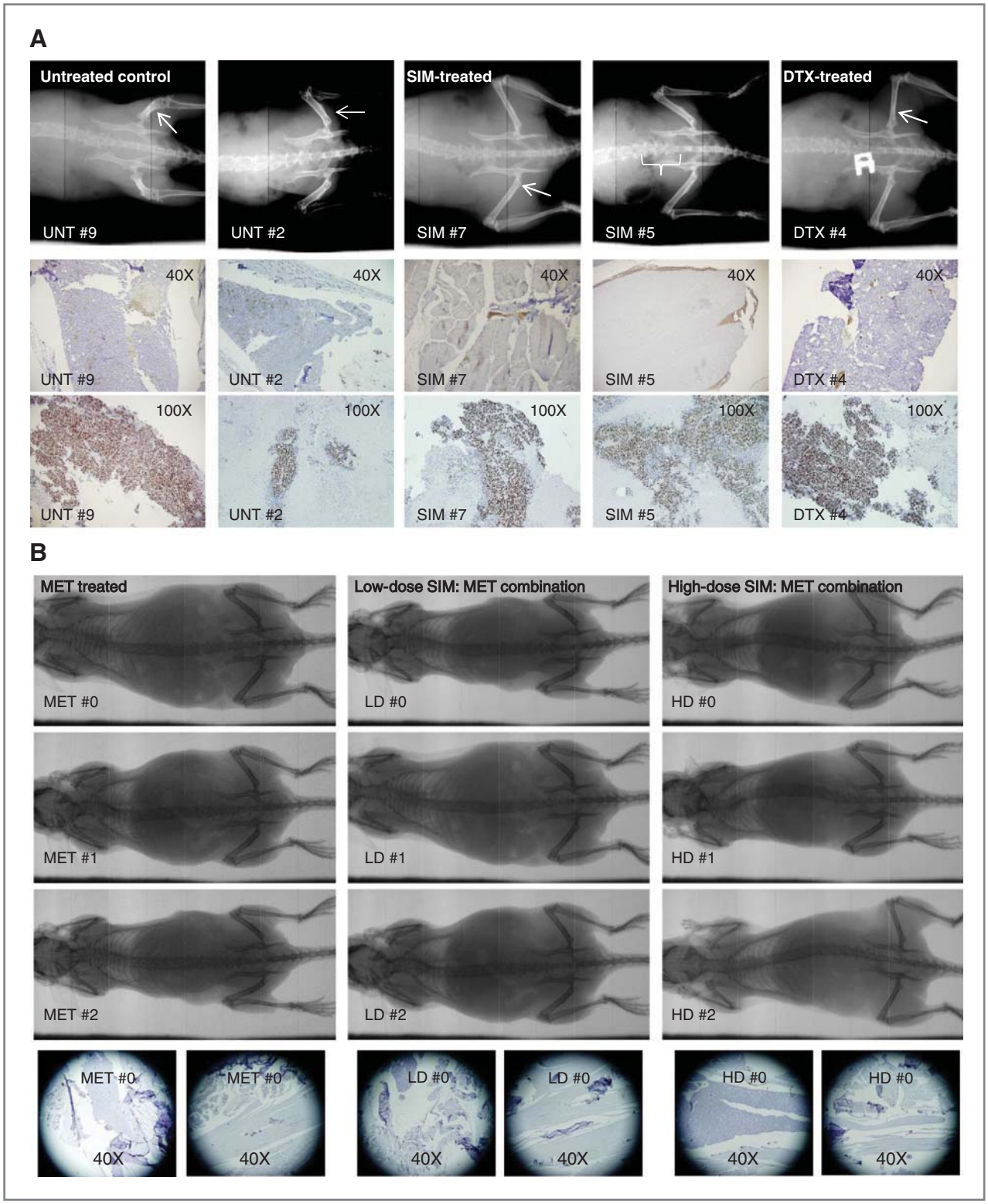

Figure 5. Metformin (MET) treatment prevents bone metastasis in C4-2B4 orthotopically inoculated mice. A, x-ray images and androgen receptor–stained IHC slides at 40× and 100× identifying C4-2B4 CRPC bone metastases in untreated (UNT) mouse #2 and mouse #9 femurs, simvastatin-treated mouse #7 femurs and mouse #5 spinal column, and docetaxel (DTX)-treated mouse #4 femurs. Arrows, clinical radiologist-identified areas of potential bone metastasis; slides were cut and androgen receptor IHC stained based on radiologist recommendation. B, representative x-ray images and androgen receptor IHC-stained slides at 40× from femurs (left) and spinal columns (right) of metformin-treated, low-dose combination (LD)–treated, and high-dose combination (HD)–treated mice. All metformin, LD, and HD slides were androgen receptor–negative.

Published OnlineFirst August 13, 2014; DOI: 10.1158/1535-7163.MCT-14-0451

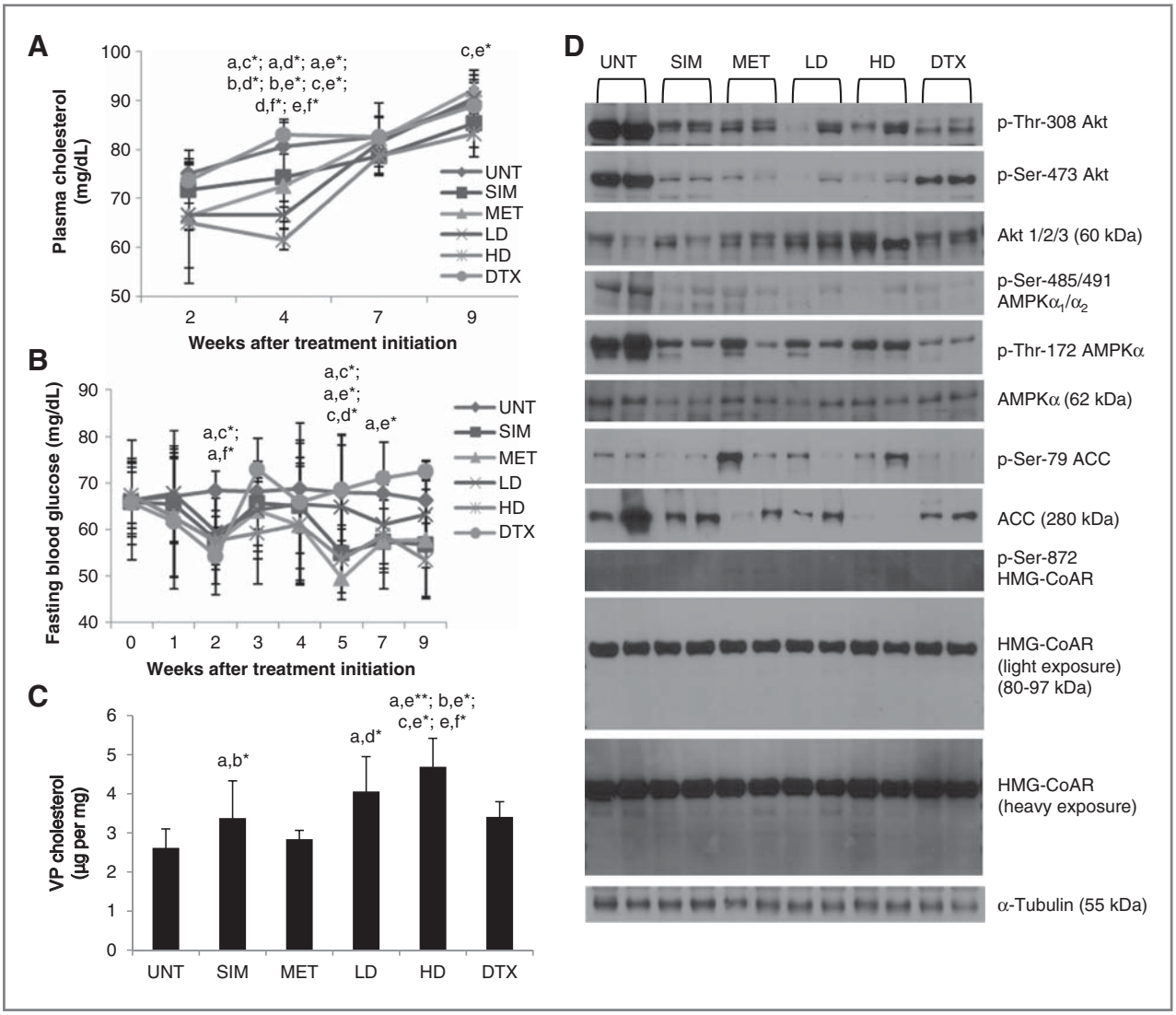

Figure 6. Combination of simvastatin (SIM) and metformin (MET) is bioavailable and mitigates altered metabolism in an orthotopic mouse model of CRPC. A, mouse plasma cholesterol (mg/dL, mean ± SD) among the six treatment groups at 2, 4, 7, and 9 weeks following treatment initiation. Overall, a significant difference was found in plasma cholesterol concentration among the six treatment groups at weeks 4 ($P < 0.0001$) and 9 ($P = 0.008$). Mouse plasma cholesterol concentration increases with age, accounting for acclivous trend. B, fasting blood glucose concentration (mg/dL, mean ± SD) among the six mouse groups at 1, 2, 3, 4, 5, 7, and 9 weeks following treatment initiation. Overall, a statistically significant difference was found in fasted blood glucose between the treatment groups at weeks 2 ($P = 0.01$), 5 ($P = 0.003$), and 9 ($P = 0.009$). C, quantification (mean ± SD) of mouse ventral prostate/tumor cholesterol concentration (µg/mg of tissue) as determined using EI-GC/MS. D, Western blot analysis of protein phosphorylation and expression of Akt, AMPKα, ACC, and HMGCR in ventral prostate/tumor tissue from representative mice of the six treatment groups; α-tubulin used as a loading control. DTX, docetaxel; HD, high-dose combination; LD, low-dose combination; UNT, untreated. Statistical significance was determined using ANOVA followed by the Tukey multiple comparison procedure. Pair-wise comparisons were depicted where UNT (a), simvastatin (b), metformin (c), LD (d), HD (e), and docetaxel (f). *, $P < 0.05$; **, $P < 0.01$; and ***, $P < 0.001$.

simvastatin, or metformin groups, and showed concomitant decrease in p-Ser485/491 AMPKα_1/α_2 and increase of Ser-79 ACC and Ser-872 HMG-CoAR phosphorylation (Fig. 6D). Despite significantly elevated ventral prostate cholesterol in the LD and HD groups, no change was noted in HMG-CoAR protein expression, with the exception of modestly increased low molecular weight cleavage products, indicative of increased negative feedback regulation (Fig. 6D). Simvastatin acid, present within ventral prostate tissue in pg/mg concentrations, significantly affects the ventral prostate cholesterol levels, perhaps through low-dose stimulation of HMG-CoAR and the hormetic bell shape of its dose–response, and metformin, despite inducing no change in ventral prostate cholesterol levels itself, does seem to amplify the simvastatin acid effect, perhaps through Ser-872 phosphorylation and indirect inhibition of HMG-CoAR activity. Changes in phosphorylation and activity of Akt, AMPKα, and HMG-CoAR, observed within the ventral prostate tissue in LD and HD groups, indicate a comparable, but not

Published OnlineFirst August 13, 2014; DOI: 10.1158/1535-7163.MCT-14-0451

identical, amelioration of metabolic aberration observed in cell culture studies.

Combination of simvastatin and metformin synergistically reduces cell viability of other models of docetaxel-resistant, hormone-refractory bone metastatic cancers

Like advanced prostate cancer, the primary site of metastasis in another hormonally regulated cancer, breast cancer, is the bone (49). Therefore, we hypothesized that simvastatin and metformin combination chemotherapy may also demonstrate a broader applicability to other models of osseous metastases, docetaxel-resistant, hormone-refractory prostate and breast cancer. PC-3 D12 is a docetaxel-resistant strain of the androgen-independent, bone metastasis–derived PC-3 PCa cell line (50). The MDA-MB-231 cell was derived from triple-negative breast cancer; the MDA-MB-231(SA) cell is a highly bone metastatic variant of the cell line MDA-MB-231 (49). PC-3 D12, MDA-MB-231, and MDA-MB-231(SA) cells demonstrate Akt, AMPKα, HMGCR, and ACC phosphorylation and protein expression patterns similar to those observed in C4-2B3/B4 omCRPC cells (Supplementary Fig. S24). In contrast with PC-3 cells, which have an IC_{50} of $\leq$2 nmol/L docetaxel, the docetaxel IC_{50} in PC-3 D12 is approximately 5.6 μmol/L (Supplementary Fig. S25A). Treatment of MDA-MB-231 and MDA-MB-231(SA) cells with docetaxel over the pharmacologic range for 24 hours only led to maximal cell viability inhibition of 21% and 34%, respectively (Supplementary Fig. S25B and S25C). Therefore, all three of these cell lines display resistance to docetaxel treatment. In contrast with docetaxel, 1:500 simvastatin and metformin combination along the pharmacologic range of 500 nmol/L to 4 μmol/L simvastatin and 250 μmol/L to 2 mmol/L metformin significantly decreased viability in all three cell lines compared with untreated control (Supplementary Fig. S25D–S25F), resulting in a viability reduction of 73% to 92% in PC-3 D12, 67% to 94% in MDA-MB-231, and 56% to 96% in MDA-MB-231(SA). Using the Chou–Talalay method, we determined that 1:500 simvastatin and metformin combination is synergistic in all three tested cell lines (Supplementary Fig. S26 and Supplementary Tables S4 and S5).

Discussion

Here, we report that combination of simvastatin and metformin acts synergistically, within the pharmacologic range, to inhibit C4-2B3/B4 mCRPC cell viability, with minimal adverse effect on PrEC normal prostate epithelial cells, prevents invasion, migration, and colony formation, and inhibits primary tumor formation, cachexia, bone metastasis, and biochemical failure in a C4-2B4 orthotopic mouse model, through amelioration of CRPC metabolic aberrations.

Treatment of mCRPC is challenging, with limited success; docetaxel remains first-line chemotherapy, yet results in frequent occurrence of docetaxel-resistant disease (3). We found pharmacologic dosages of docetaxel indiscriminately toxic to normal prostate epithelial cells, at concentrations as low as 10 nmol/L; yet, all mCRPC sublines used within this study exhibited resistance to docetaxel-induced inhibition of cell viability. Docetaxel at 24 μg/g body weight dose was highly toxic to mice as 75% of animals experienced systemic toxicity and bowel obstruction, due to docetaxel effect on dividing cells within intestinal tissue, leading to mortality. This dosage was chosen to simulate the human treatment regimen and for maximal efficacy on C4-2B4 cells; a lower dose may have resulted in less systemic toxicity to the mice, but may have also reduced inhibition of CRPC tumor growth and metastasis. Patients often discontinue docetaxel use due to side effects, such as secondary infections and fever due to neutropenia and immuno-depression, anemia, edema, peripheral neuropathy, allergic reactions, weakness, and development of docetaxel-resistant disease (3, 4).

Our preclinical results suggest that combination of simvastatin and metformin may be an effective, convenient, inexpensive, and less toxic alternate chemotherapeutic option for the treatment of mCRPC. Using CompuSyn software, we determined that 1:500 simvastatin and metformin combination is synergistic and was found to significantly inhibit viability and metastatic properties of C4-2B3/B4 cells more effectively than docetaxel, simvastatin, or metformin treatment alone, with minimal adverse effect on PrEC cells. In an orthotopic model of mCRPC, combination of simvastatin and metformin, at dosages equivalent to low-to-mid range for the treatment of hypercholesterolemia and T2D, completely inhibited C4-2B4 primary tumor growth, significantly reduced GU weight and ventral prostate tissue PCNA protein expression, completely inhibited cachexic wasting, metastasis to bone, and prevented biochemical failure, significantly better than simvastatin or metformin alone or docetaxel chemotherapy, without adversely affecting animal health. Simvastatin and metformin combination treatment abated metabolic aberrations noted in the C4-2B3/B4 mCRPC cells in a time-dependent fashion, decreasing Akt Ser-473 and Thr-308 phosphorylation, leading to a reduction of inhibitory p-Ser-485/491 of AMPKα_1/α_2, and simultaneously increasing Thr-172 phosphorylation and AMPKα kinase activity. Simvastatin and metformin combination treatment also inhibited HMG-CoAR activity and significantly diminished cellular cholesterol concentration in mCRPC cells to levels comparable with those found in RWPE-1 cells. Amelioration of metabolic aberrations was also noted in *in vivo* studies, at both systemic level and directly in the ventral prostate tissue, where combination treatment reduced Akt phosphorylation and increased AMPKα catalytic activity. Whether amelioration of these metabolic aberrations (and potential inhibition of aerobic glycolysis and biomass production) is the mechanism by which simvastatin and metformin treatment selectively kills CRPC cells and not normal epithelial cells warrants further investigation.

Published OnlineFirst August 13, 2014; DOI: 10.1158/1535-7163.MCT-14-0451

Presently, an ongoing clinical trial (http://clinicaltrials.gov/ct2/show/NCT01561482) is investigating the use of simvastatin and metformin combination for the prevention of rising PSA following radical prostatectomy or radiotherapy for localized prostate cancer. This trial does not directly address the effect of simvastatin and metformin combination in CRPC (as patients on ADT within 6 months before study enrollment are not eligible) or in metastatic disease (as subjects can only participate until metastatic progression). Provided the investigators account for patients with and without previous ADT use during data analysis, it will be interesting to know whether simvastatin and metformin combination chemotherapy demonstrates different efficacies with respect to hormone-dependent and hormone-refractory cancers, because the same metabolic aberrations noted in CRPC and advanced bone metastatic prostate cancer were not identified in early androgen-dependent prostate cancer in our study (AMPKα still active, HMG-CoAR still demonstrate normal negative feedback regulation, and less cholesterol accumulation). Without accounting for previous ADT use, beneficial effects of simvastatin and metformin combination chemotherapy may remain unseen within this clinical trial, as simvastatin and metformin combination treatment may be more effective in patients with CRPC.

Our *in vitro* experimentation in PC-3 D12, MDA-MB-231, and MDA-MB-231(SA) cell lines suggests that simvastatin and metformin combination may have broader applicability as a therapeutic option for metastatic docetaxel-resistant prostate cancer and triple-negative breast cancer. These cell lines demonstrate altered metabolism, similar to that observed in the C4-2B strains, and could explain why simvastatin and metformin treatment is effective in these cells. Furthermore, of interest would be investigation as to whether simvastatin and metformin combination treatment could translate to other bone metastatic cancers, such as carcinoma of the lungs or kidneys.

With respectable safety profiles, simvastatin and metformin combination treatment could be readily used by elderly patients and those who cannot tolerate or fail docetaxel. Simvastatin and metformin are oral drugs consumed daily, facilitating ease of use, in contrast with other expensive FDA-approved chemotherapeutic drugs. In conclusion, our studies have identified an effective, inexpensive alternate chemotherapy with an excellent safety record that would greatly benefit quality of life of patients with mCRPC and perhaps other cancers metastasizing to bone.

Disclosure of Potential Conflicts of Interest

No potential conflicts of interest were disclosed.

Authors' Contributions

Conception and design: M.A. Babcook, S. Gupta
Development of methodology: M.A. Babcook, S. Shukla, E.J. Vazquez, M.A. Puchowicz, D.J. Lindner
Acquisition of data (provided animals, acquired and managed patients, provided facilities, etc.): M.A. Babcook, E.J. Vazquez, M.A. Puchowicz, J.P. Molter, C.Z. Oak, C.A. Flask, D.J. Lindner, Y. Parker, F. Daneshgari
Analysis and interpretation of data (e.g., statistical analysis, biostatistics, computational analysis): M.A. Babcook, P. Fu, M.A. Puchowicz, G.T. MacLennan
Writing, review, and/or revision of the manuscript: M.A. Babcook, C.A. Flask, D.J. Lindner, S. Gupta
Administrative, technical, or material support (i.e., reporting or organizing data, constructing databases): M.A. Puchowicz, F. Daneshgari, S. Gupta
Study supervision: S. Shukla, M.A. Puchowicz, D.J. Lindner, S. Gupta

Acknowledgments

The authors thank Dr. Robert A. Sikes of the Center for Translational Cancer Research, University of Delaware (Newark, DE); Dr. Bill Watson of the Conway Institute of Biomolecular and Biomedical Research, University College Dublin, Ireland; Dr. Theresa Guise of the Department of Medicine, Indiana University School of Medicine (Indianapolis, IN); and Dr. Hung-Ying Kao of the Department of Biochemistry, Case Western Reserve University School of Medicine (Cleveland, OH) for gifts of cell lines. They also thank Dr. Hung-Ying Kao, Dr. Henri Brunengraber, and the CWRU MMPC (U24DK76174) for use of equipment and reagents necessary for completion of this work. They also thank David DeSantis and Chih-Wei Ko for their assistance and expertise with the ALT assay, and Dr. Colleen Croniger for use of the kinetic spectrophotometer necessary for completion of this assay. They greatly appreciate Dr. Christopher J. Hoimes for providing suggestions for editing and revision of the article.

Grant Support

This work was supported by NIH R01CA10852 (awarded to S. Gupta), Urology Vision Research Funds, and the Clinical and Translational Science Collaborative (CTSC) of Cleveland UL1TR000439 from the National Center for Advancing Translational Sciences (NCATS) component of the NIH and NIH Roadmap for Medical Research. M.A. Babcook was supported by NIH 5T32DK007319 Ruth L. Kirschstein Pre-Doctoral Fellowship through the Metabolism Training Program.

The costs of publication of this article were defrayed in part by the payment of page charges. This article must therefore be hereby marked *advertisement* in accordance with 18 U.S.C. Section 1734 solely to indicate this fact.

Received May 29, 2014; revised July 21, 2014; accepted August 3, 2014; published OnlineFirst August 13, 2014.

References

1. Garcia JA, Rini BI. Castration-resistant prostate cancer: many treatments, many options, many challenges ahead. Cancer 2012;118:2583–93.
2. Liu JJ, Zhang J. Sequencing systemic therapies in metastatic castration-resistant prostate cancer. Cancer Control 2013;20:181–7.
3. Singer EA, Srinivasan R. Intravenous therapies for castration-resistant prostate cancer: toxicities and adverse events. Urol Oncol 2012;30:S15–9.
4. El-Amm J, Aragon-Ching JB. The changing landscape in the treatment of metastatic castration-resistant prostate cancer. Ther Adv Med Oncol 2013;5:25–40.
5. Thysell E, Surowiec I, Hörnberg E, Crnalic S, Widmark A, Johansson AI, et al. Metabolomic characterization of human prostate cancer bone metastases reveals increased levels of cholesterol. PLos ONE 2010;5:e14175.
6. Kreisberg JI, Malik SN, Prihoda TJ, Bedolla RG, Troyer DA, Kreisberg S, et al. Phosphorylation of Akt (Ser473) is an excellent predictor of poor clinical outcome in prostate cancer. Cancer Res 2004;64:5232–6.
7. Mulholland DJ, Tran LM, Li Y, Cai H, Morim A, Wang S, et al. Cell autonomous role of PTEN in regulating castration-resistant prostate cancer growth. Cancer Cell 2011;19:792–804.
8. Klop B, Elte JW, Cabezas MC. Dyslipidemia in obesity: mechanisms and potential targets. Nutrients 2013;5:1218–40.
9. Mondul AM, Clipp SL, Helzlsouer KJ, Platz EA. Association between plasma total cholesterol concentration and incident

Published OnlineFirst August 13, 2014; DOI: 10.1158/1535-7163.MCT-14-0451

prostate cancer in the CLUE II cohort. Cancer Causes Control 2010;21:61–8.
10. Moreira DM, Anderson T, Gerber L, Thomas JA, Bañez LL, McKeever MG, et al. The association of diabetes mellitus and high-grade prostate cancer in a multiethnic biopsy series. Cancer Causes Control 2011;22:977–83.
11. Mondul AM, Weinstein SJ, Virtamo J, Albanes D. Serum total and HDL cholesterol and risk of prostate cancer. Cancer Causes Control 2011;22:1545–52.
12. Moses KA, Utuama OA, Goodman M, Issa MM. The association of diabetes and positive prostate biopsy in a US veteran population. Prostate Cancer Prostatic Dis 2012;15:70–4.
13. Krycer JR, Brown AJ. Cholesterol accumulation in prostate cancer: a classic observation from a modern perspective. Biochim Biophys Acta 2013;1835:219–29.
14. Gunter JH, Sarkar PL, Lubik AA, Nelson CC. New players for advanced prostate cancer and the rationalization of insulin-sensitizing medication. Int J Cell Biol 2013;2013:834684.
15. Gutt R, Tonlaar N, Kunnavakkam R, Karrison T, Weichselbaum RR, Liauw SL. Statin use and risk of prostate cancer recurrence in men treated with radiation therapy. J Clin Oncol 2012;28:2653–9.
16. Hamilton RJ, Banez LL, Aronson WJ, Terris MK, Platz EA, Kane CJ, et al. Statin medication use and the risk of biochemical recurrence after radical prostatectomy: results from the Shared Equal Access Regional Cancer Hospital (SEARCH) database. Cancer 2010;116:3389–98.
17. Marcella SW, David A, Ohman-Strickland PA, Carson J, Rhoads GG. Statin use and fatal prostate cancer: a matched case-control study. Cancer 2012;118:4046–52.
18. Spratt DE, Zhang C, Zumsteg ZS, Pei X, Zhang Z, Zelefsky MJ. Metformin and prostate cancer: reduced development of castration-resistant disease and prostate cancer mortality. Eur Urol 2013;63:709–16.
19. Zannella VE, Dal Pra A, Muaddi H, McKee TD, Stapleton S, Sykes J, et al. Reprogramming metabolism with metformin improves tumor oxygenation and radiotherapy response. Clin Cancer Res 2013;19:6741–50.
20. Jespersen CG, Nørgaard M, Friis S, Skriver C, Borre M. Statin use and risk of prostate cancer: a Danish population-based case-control study, 1997–2010. Cancer Epidemiol 2014;38:42–7.
21. Lehman DM, Lorenzo C, Hernandez J, Wang CP. Statin use as a moderator of metformin effect on risk for prostate cancer among type 2 diabetic patients. Diabetes Care 2012;35:1002–7.
22. Hoque A, Chen H, Xu XC. Statin induces apoptosis and cell growth arrest in prostate cancer cells. Cancer Epidemiol Biomarkers Prev 2008;17:88–94.
23. Ben Sahra I, Laurent K, Loubat A, Giorgetti-Peraldi S, Colosetti P, Auberger P, et al. The antidiabetic drug metformin exerts an antitumoral effect in vitro and in vivo through a decrease of cyclin D1 level. Oncogene 2008;27:3576–86.
24. Kochuparambil ST, Al-Husein B, Goc A, Soliman S, Somanath PR. Anticancer efficacy of simvastatin on prostate cancer cells and tumor xenografts is associated with inhibition of Akt and reduced prostate-specific antigen expression. J Pharmacol Exp Ther 2011;336:496–505.
25. Brown M, Hart C, Tawadros T, Ramani V, Sangar V, Lau M, et al. The differential effects of statins on the metastatic behaviour of prostate cancer. Br J Cancer 2012;106:1689–96.
26. Avci CB, Harman E, Dodurga Y, Susluer SY, Gunduz C. Therapeutic potential of an anti-diabetic drug, metformin: alteration of miRNA expression in prostate cancer cells. Asian Pac J Cancer Prev 2013;14:765–8.
27. Rosing H, Lustig V, van Warmerdam LJ, Huizing MT, ten Bokkel Huinink WW, Schellens JH, et al. Pharmacokinetics and metabolism of docetaxel administered as a 1-h intravenous infusion. Cancer Chemother Pharmacol 2000;45:213–8.
28. Bederman IR, Foy S, Chandramouli V, Alexander JC, Previs SF. Triglyceride synthesis in epididymal adipose tissue: contribution of glucose and non-glucose carbon sources. J Biol Chem 2009;284:6101–8.
29. Shukla S, Bhaskaran N, Babcook MA, Fu P, MacLennan GT, Gupta S. Apigenin inhibits prostate cancer progression in TRAMP mice via targeting PI3K/Akt/FoxO pathway. Carcinogenesis 2014;35:452–60.
30. Chou TC. Theoretical basis, experimental design, and computerized simulation of synergism and antagonism in drug combination studies. Pharmacol Rev 2006;58:621–81.
31. Liang CC, Park AY, Guan JL. In vitro scratch assay: a convenient and inexpensive method for analysis of cell migration in vitro. Nat Protoc 2007;2:329–33.
32. Marshall J. Transwell invasion assays. Methods Mol Biol 2011;769: 97–110.
33. Gupta A, Mehta R, Alimirah F, Peng X, Murillo G, Wiehle R, et al. Efficacy and mechanism of action of Proellex, an antiprogestin in aromatase overexpressing and Letrozole resistant T47D breast cancer cells. J Steroid Biochem Mol Biol 2013;133:30–42.
34. Fang D, West RH, Manson ME, Ruddy J, Jiang D, Previs SF, et al. Increased plasma membrane cholesterol in cystic fibrosis cells correlates with CFTR genotype and depends on the de novo cholesterol synthesis. Respir Res 2010;11:61.
35. Morris MJ, Gilbert JD, Hsieh JY, Matuszewski BK, Ramjit HG, Bayne WF. Determination of the HMG-CoA reductase inhibitors simvastatin, lovastatin, and pravastatin in plasma by gas chromatography/chemical ionization mass spectrometry. Biol Mass Spectrom 1993;22:1–8.
36. Zhang J, Rodila R, Gage E, Hautman M, Fan L, King LL, et al. High-throughput salting-out assisted liquid/liquid extraction with acetonitrile for the simulataneous determination of simvastatin and simvastatin acid in human plasma with liquid chromatography. Anal Chim Acta 2010;661:167–72.
37. Uçaktürk E. The development and validation of a gas chromatography-mass spectrometry method for the determination of metformin in human plasma. Anal Methods 2013;5:4723–30.
38. Thalmann GN, Sikes RA, Wu TT, Degeorges A, Chang SM, Ozen M, et al. LNCaP progression model of human prostate cancer: androgen-independence and osseous metastasis. Prostate 2000;44:91–103.
39. Krycer JR, Brown AJ. Does changing androgen receptor status during prostate cancer development impact upon cholesterol homeostasis? PLoS ONE 2013;8:e54007.
40. Russo GL, Russo M, Ungaro P. AMP-activated protein kinase: a target for old drugs against diabetes and cancer. Biochem Pharmacol 2013;86:339–50.
41. Zhou G, Myers R, Li Y, Chen Y, Shen X, Fenyk-Melody J, et al. Role of AMP-activated protein kinase in mechanism of metformin action. J Clin Invest 2001;108:1167–74.
42. Soltys CLM, Kovacic S, Dyck JRB. Activation of cardiac AMP-activated protein kinase by LKB1 expression or chemical hypoxia is blunted by increased Akt activity. Am J Physiol Heart Circ Physiol 2006;290:H2472–9.
43. Kayampilly PP, Menon KM. Follicle-stimulating hormone inhibits adenosine 5′-monophosphate-activated protein kinase activation and promotes cell proliferation of primary granulosa cells in culture through an Akt-dependent pathway. Endocrinology 2009;150:929–35.
44. Pulinilkunnil T, He H, Kong D, Asakura K, Peroni OD, Lee A, et al. Adrenergic regulation of AMP-activated protein kinase in brown adipose tissue in vivo. J Biol Chem 2011;286:8798–809.
45. Caino MC, Chae YC, Vaira V, Ferrero S, Nosotti M, Martin NM, et al. Metabolic stress regulates cytoskeletal dynamics and metastasis of cancer cells.J Clin Invest 2013;123:2907–20.
46. Park HJ, Kong D, Iruela-Arispe L, Begley U, Tang D, Galper JB. 3-hydroxy-3-methylglutaryl coenzyme A reductase inhibitors interfere with angiogenesis by inhibiting the geranylgeranylation of RhoA. Circ Res 2002;91:143–50.
47. Di Buono M, Jones PJH, Beaumier L, Wykes LJ. Comparison of deuterium incorporation and mass isotopomer distribution analysis for measurement of human cholesterol biosynthesis. J Lipid Res 2000;41:1516–23.
48. Mener DJ. Prostate specific antigen reduction following statin therapy: mechanism of action and review of the literature. IUBMB Life 2010; 62:584–90.
49. Pollari S, Käkönen SM, Edgren H, Wolf M, Kohonen P, Sara H, et al. Enhanced serine production by bone metastatic breast cancer cells stimulates osteoclastogenesis. Breast Cancer Res Treat 2011;125: 421–30.
50. O'Neill AJ, Prencipe M, Dowling C, Fan Y, Mulrane L, Gallagher WM, et al. Characterization and manipulation of docetaxel resistant prostate cancer cell lines. Mol Cancer 2011;10:126.